J. Fluid Mech. (1986), *vol.* 162, *pp.* 187–209
Printed in Great Britain

On the gradual reflection of weakly nonlinear Stokes waves in regions with varying topography

By JAMES T. KIRBY

Coastal & Oceanographic Engineering Department, University of Florida, Gainesville, FL 32611

(Received 7 August 1984 and in revised form 18 July 1985)

Coupled equations governing the forward- and back-scattered components of a linear wave propagating in a region with varying depth may be derived from a second-order wave equation for linear wave motion. In this paper previous studies are extended to the case of weakly nonlinear Stokes waves coupled at third order in wave amplitude, using a Lagrangian formulation for irrotational motions. Comparison with previous computational and experimental results are made.

1. Introduction

Various recent studies have explored the application of the parabolic-equation method to the problems of wave propagation in a slowly varying domain. In the linear wave approximation, Berkhoff (1972) has provided a second-order wave equation governing the surface potential $\hat{\phi}(x, y)$ of a harmonic wave, based on the assumption of modulation lengthscales smaller than the wave-steepness scale. Radder (1979) obtained coupled parabolic equations for forward- and back-scattered waves, where it is assumed that both waves travel at a small angle to a prespecified direction. A model for the forward-scattered wave field alone is then obtained by neglecting the coupling terms. Berkhoff, Booij & Radder (1982) have provided a data set for wave amplitude in an area of waves focused by a submerged shoal, and have used the data to test Radder's model. Additional results for forward scattering alone in a linear approximation have been provided by Liu & Mei (1976) and Tsay & Liu (1982). Kirby & Dalrymple (1983) have extended the linear wave approximation to include the effect of cubic nonlinearity for Stokes waves, which leads to a nonlinear Schrödinger equation for the wave amplitude. Kirby & Dalrymple (1984) have tested the nonlinear model in comparison with the data set of Berkhoff, Booij & Radder and have shown a distinct improvement in agreement between model and data in comparison to the results of Radder's model. The nonlinear model has thus been shown to be a relevant addition to the study of combined refraction–diffraction.

The results mentioned above are based on the assumption that the reflected wave is absent or negligible. This assumption is certainly valid locally in a slowly varying domain; however, a sizeable reflected component may accumulate for waves propagating over long distances or over fairly abrupt obstacles. Liu & Tsay (1983) have developed an iterative scheme based on coupled equations similar to those of Radder (1979), and have shown that the coupled method for forward- and back-scattered waves is capable of producing results in agreement with a finite-element solution of Berkhoff's equation, where the entire wavefield is calculated simultaneously (Tsay & Liu 1983).

In a separate development, Kirby (1986) has shown that Berkhoff's equation may

be simply extended to include the case of bottom undulations with lengthscales on the order of a wavelength but with small amplitude relative to their wavelength. This extension allows for the direct calculation of relatively stronger reflections due to Bragg scattering between the surface waves and bed undulations. These reflections may be strong even in intermediate water depths, and hence are well suited for consideration in the present investigation.

In this study, we extend the results of Kirby & Dalrymple (1983), Liu & Tsay (1983) and Kirby (1985) to study the gradual reflection of Stokes waves by depth variations. In §2, a derivation of the equations governing the evolution of a slowly varying partial standing wavetrain are derived in order to obtain the nonlinear coupling coefficients between incident and reflected waves. Section 3 then presents a splitting approach which produces the set of coupled parabolic equations needed. In §4, we study a special case of waves normally incident on topography varying in one direction, in order to evaluate the effect of neglecting interaction with wave-induced currents which enter the equations at third order. The parabolic approximation is then applied to the study of a two-dimensional problem in §5.

2. Derivation of the equations governing wave propagation

We wish to derive the equations governing the forward- and backward-moving wave components in a partial standing wave, where x is taken as the (positive) direction of travel. Previous derivations of the nonlinear Schrödinger equation for forward-scattered waves alone have relied on the WKB formulation and a multiple-scale expansion of the governing equations. However, a scheme for providing coupled equations has not been devised using that approach. Here, we will rely instead on a variational formulation using the Lagrangian for irrotational motion of an inviscid fluid, given by Luke (1967). After deriving equations for a general wave motion in two horizontal dimensions (x, y) and time, the results will be specialized to the case of two waves propagating in an antiparallel direction. The method used here is further discussed in Kirby (1983) in connection with the problem of wave–current interaction.

2.1. *The Lagrangian formulation and governing equations*

The Lagrangian for irrotational motion is given by (Luke 1967)

$$L = \int_{-h}^{\eta} \rho \{\phi_t + \tfrac{1}{2}(\nabla_h \phi)^2 + \tfrac{1}{2}(\phi_z)^2 + gz\} \, \mathrm{d}z. \tag{2.1}$$

Here, $\eta(x, y, t)$ is the instantaneous position of the water surface with respect to still water level $z = 0$, and $h(x, y)$ is the local water depth. The potential $\phi(x, y, z, t)$ is related to the fluid velocity according to

$$\boldsymbol{u} = \nabla \phi, \tag{2.2}$$

Further, ∇_h denotes a horizontal gradient vector $\{\partial/\partial x, \partial/\partial y\}$ and subscripts denote differentiation. The corresponding variational principle is given by

$$\delta \int_t \int_x L \, \mathrm{d}\boldsymbol{x} \, \mathrm{d}t = 0, \tag{2.3}$$

where the integration is over the propagation space $\{x, y, t\}$.

Since we wish to study the spatial evolution of a time-independent wavefield, it is sufficient to chose forms for ϕ and η based on a slow-modulation solution of the

governing equations, as in Whitham (1967). Consequently, we choose a wave-steepness scale ϵ and modulation scale μ and propose *a priori* that $\mu \approx \epsilon^2$. This assumption produces a mild-slope approximation as in Kirby & Dalrymple (1983). We choose ϕ and η according to

$$\phi = \epsilon f_1(\mu x, z)\,\tilde{\phi}_1(x,t) + \epsilon^2\left\{f_2(\mu x, z)\,\tilde{\phi}_2(x,t) + \phi_2'(x,\mu t) - \int \gamma_2(\mu x, t)\,\mathrm{d}t\right\}, \quad (2.4a)$$

$$\eta = \epsilon\eta_1(x,t) + \epsilon^2\{\eta_2(x,t) + b_2(x,\mu t)\}. \quad (2.4b)$$

Here, $\tilde{\phi}_1, \eta_1, \tilde{\phi}_2, \eta_2$ correspond to first- and second-order wavelike components, ϕ_2' is the potential for wave-induced mean flow, b_2 represents the wave-induced set-down, and γ_2 is related to the Bernoulli constant. We remark that in a partial standing wave γ_2 cannot be trivially eliminated by choice of b_2, and that γ_2, b_2 and ϕ_2' may have fast variations as indicated. The quantities f_1 and f_2 are given by

$$f_1 = \frac{\cosh k(h+z)}{\cosh kh}; \quad f_2 = \frac{\cosh 2k(h+z)}{\sinh^4 kh}; \quad h = h(\mu x). \quad (2.5)$$

Substituting (2.4) in (2.1) and performing the integration results in the expression

$$\begin{aligned} L = {} & \tfrac{1}{2}g(\eta^2 + h^2) + \epsilon I_1\,\tilde{\phi}_{1t} + \epsilon^2\{I_2\,\tilde{\phi}_{2t} + (h+\eta)\,(\phi_{2t}' - \gamma_2)\} \\ & + \epsilon^2 I_{1,1}\,\tfrac{1}{2}(\nabla_h\tilde{\phi}_1)^2 + \epsilon^3\{I_{1,2}\,\nabla_h\tilde{\phi}_1\cdot\nabla_h\tilde{\phi}_2 + I_1\,\nabla_h\tilde{\phi}_1\cdot\nabla_h\phi_2'\} \\ & + \epsilon^4\{I_{2,2}\,\tfrac{1}{2}(\nabla_h\tilde{\phi}_2)^2 + I_2\,\nabla_h\tilde{\phi}_2\cdot\nabla_h\phi_2' + \tfrac{1}{2}(\nabla_h\phi_2')^2\,(h+\eta)\} \\ & + \epsilon^2 I_{1,1}^z\,\tfrac{1}{2}(\tilde{\phi}_1)^2 + \epsilon^3 I_{1,2}^z\,\tilde{\phi}_1\tilde{\phi}_2 + \epsilon^4 I_{2,2}^z\,\tfrac{1}{2}(\tilde{\phi}_2)^2. \end{aligned} \quad (2.6)$$

The integrals I are over the total depth and are defined in Appendix A. The I's may be expanded about $z = 0$ in Taylor series according to

$$I = I' + \epsilon\eta_1 I'' + \epsilon^2\{(\eta_2 + b_2)\,I'' + \eta_1^2 I'''\} + \epsilon^3\{2\eta_1(\eta_2 + b_2)\,I''' + \eta_1^3 I^{\mathrm{iv}}\} + O(\epsilon^4), \quad (2.7)$$

as shown in Appendix A. Substituting the expansions in (2.6), expanding the remaining appearances of η, and retaining terms to $O(\epsilon^4)$ leads to the expression

$$L = L_0 + \epsilon L_1 + \epsilon^2 L_2 + \epsilon^3 L_3 + \epsilon^4 L_4. \quad (2.8)$$

The individual coefficients L_i are given in Appendix B. This ordering has also been utilized by Dysthe (1974) after averaging L over the phase function according to Whitham's method. Several properties of (2.8) with respect to the desired governing equations can be mentioned. Since variation with respect to a dependent parameter will reduce the order of L by the order of that parameter, it is clear that the linear equation governing the behaviour of a parameter of $O(\epsilon^n)$ will come from the variation of L_{2n} with respect to that parameter. Thus the linear equation governing $\tilde{\phi}_1$ will be contributed by L_2, while L_4 will contribute the $O(\epsilon^3)$ terms in phase with $\tilde{\phi}_1$.

We now derive governing equations which are generally applicable to any motion described by the potential (2.4*a*); L_0 and L_1 contribute nothing in this approximation. The linear wave equation is derived by first varying L_2 with respect to η_1, yielding

$$\eta_1 = -\frac{1}{g}\,\tilde{\phi}_{1t}, \quad (2.9)$$

the free-surface boundary condition. Varying L_2 with respect to $\tilde{\phi}_1$ and performing a partial integration over the propagation space yields

$$-\eta_{1t} - \nabla_h\cdot(I_{1,1}'\,\nabla_h\tilde{\phi}_1) + I_{1,1}^{z'}\,\tilde{\phi}_1 = 0. \quad (2.10)$$

Eliminating η_1 between (2.9) and (2.10) and inserting the values of the integrals yields

$$\tilde{\phi}_{1tt} - \nabla_h \cdot (CC_g \nabla_h \tilde{\phi}_1) + (\omega^2 - k^2 CC_g)\tilde{\phi}_1 = 0, \tag{2.11}$$

which is the time-dependent form of the mild-slope equation of Berkhoff (1972). Here,

$$C = \frac{\omega}{k}; \quad C_g = \frac{\partial \omega}{\partial k}; \quad \omega^2 = gk \tanh kh. \tag{2.12}$$

Varying L_4 with respect to $(\eta_2 + b_2)$ yields a free-surface boundary condition, which may be written as

$$\eta_2 + b_2 - \frac{\gamma_2}{g} = -\frac{\phi_2'}{g} - \frac{I_2''}{g}\tilde{\phi}_{2t} + \frac{2I_1'''}{g^2}(\tilde{\phi}_{1t})^2 - \frac{I_{1,1}''}{2g}(\nabla_h \tilde{\phi}_1)^2 - \frac{I_{1,1}^{z''}}{2g}\tilde{\phi}_1^2 \tag{2.13}$$

after eliminating η_1 according to (2.9). Variation of L_4 with respect to ϕ_2' and partial integration yields a continuity equation

$$(\eta_2 + b_2)_t + \nabla_h \cdot (h \nabla \phi_2') - \frac{1}{g}\nabla_h \cdot (\tilde{\phi}_{1t} \nabla_h \tilde{\phi}_1) + \nabla_h \cdot (I_2' \nabla_h \tilde{\phi}_2) = 0. \tag{2.14}$$

$(\eta_2 + b_2)$ may be eliminated between (2.13) and (2.14) to yield a forced-wave equation for the quasi-steady motion ϕ_2' after averaging over the phase.

The equation containing the nonlinear modification to the linear wave equation (2.11) may be obtained by varying $L_2 + L_4$ together by η_1 and $\tilde{\phi}_1$ and eliminating η_1, yielding

$$\epsilon\{\tilde{\phi}_{1tt} - \nabla_h \cdot (CC_g \nabla_h \tilde{\phi}_1) + (\omega^2 - k^2 CC_g)\tilde{\phi}_1\} = \epsilon^3\{\text{N.L.T.}\} \tag{2.15}$$

{N.L.T.} is a complicated expression involving products of $\tilde{\phi}_1$, $(\eta_2 + b_2)$, $\tilde{\phi}_2$ and ϕ_2', and is given in Appendix C for completeness. We remark that terms in {N.L.T.} have been manipulated by substitution using the linearized relationships, in analogous form to the treatment of higher-order terms in the Boussinesq wave formulation. Equation (2.15) is in the form of a second-order hyperbolic equation for a general wave motion in $\{x, y, t\}$; however, {N.L.T.} contains components proportional to the third harmonic $\tilde{\phi}_3$. These terms are eliminated in the derivation of the evolution equations. An equation similar to (2.15) has been given previously by Liu & Tsay (1984) for the case of progressive waves.

2.2. *Explicit results for partial standing waves*

We now wish to construct parabolic approximations for the amplitude of two wave components of the same frequency ω and with an angle of 180° between the assumed direction of the wavenumber vectors. We choose

$$\begin{aligned}\tilde{\phi}_1 &= \phi_1^+ + \phi_1^- \\ &= -\frac{ig}{2\omega} A(\mu x, \mu y, \mu t) E_+ + * - \frac{ig}{2\omega} B(\mu x, \mu y, \mu t) E_- + *,\end{aligned} \tag{2.16}$$

where

$$E_+ = \exp\left[i\left(\int k(x)\,dx - \omega t\right)\right]; \quad E_- = \exp\left[i\left(-\int k(x)\,dx - \omega t\right)\right]; \quad \omega^2 = gk \tanh kh, \tag{2.17}$$

and where * denotes the complex conjugate of the preceding term. The propagation

direction of ϕ^+ is oriented with the $+x$-direction. Using this splitting and the equations of the preceding subsection, we obtain

$$\eta_1 = \frac{A}{2} E_+ + * + \frac{B}{2} E_- + * + O(\mu), \tag{2.18}$$

$$\tilde{\phi}_2 = -\frac{3i\omega}{16} A^2 E_+^2 + * - \frac{3i\omega}{16} B^2 E_-^2 + * + O(\mu), \tag{2.19}$$

$$\eta_2 = \tfrac{1}{4}k \frac{\cosh 2kh - 2}{\sinh 2kh} \{A^2 E_+^2 + B^2 E_-^2 + *\} - \frac{I_2''}{g} \tilde{\phi}_{2t}$$

$$= \tfrac{1}{8}k \frac{\cosh kh(\cosh 2kh + 2)}{\sinh^3 kh} \{A^2 E_+^2 + B^2 E_-^2 + *\} + O(\mu), \tag{2.20}$$

$$b_2 = -\frac{1}{g} \phi_{2t}' - \frac{k(|A|^2 + |B|^2)}{2 \sinh 2kh} + \frac{k \cosh 2kh}{2 \sinh 2kh} (AB^* E_+ E_-^* + *). \tag{2.21}$$

The third term in (2.21) corresponds to a rapid standing variation at $\cos(2kx)$ corresponding to the envelope of the partial standing wave. Further,

$$\gamma_2 = \frac{-gk(2 \cosh 2kh - 1)}{2 \sinh 2kh} \{ABE_+ E_- + *\}, \tag{2.22}$$

which represents a spatially slowly varying oscillation at $\cos(2\omega t)$. We remark that γ_2 may not be eliminated by choice of b_2, in contrast to the progressive-wave problem. Elimination of $(\eta_2 + b_2)$ between (2.13) and (2.14) yields the forced-wave equation for the $O(\epsilon^2)$ mean motion:

$$\phi_{2tt}' - \nabla_h \cdot (gh \nabla_h \phi_2') = \frac{g^2}{2\omega} (k|A|^2 - k|B|^2)_x - \frac{gk}{2 \sinh 2kh} (|A|^2 + |B|^2)_t$$

$$+ \frac{gk \cosh 2kh}{2 \sinh 2kh} (AB^* E_+ E_- + *)_t. \tag{2.23}$$

The third term on the right-hand side of (2.23) indicates that spatially fast ($\sim 2kx$) adjustments in b_2 and ϕ_2' will occur in response to slow temporal changes in the amplitude of ϕ_1^+ or ϕ_1^-.

Substitution of (2.16)–(2.21) in the expression for N.L.T. yields the result

$$\text{N.L.T.} = -2\omega \left\{ k\phi_{2x}' - \frac{k^2}{2\omega \cosh^2 kh} \phi_{2t}' \right\} \phi_1^+ + 2\omega \left\{ k\phi_{2x}' + \frac{k^2}{2\omega \cosh^2 kh} \phi_{2t}' \right\} \phi_1^-$$

$$- \omega^2 k^2 D_1 (|A|^2 \phi_1^+ + |B|^2 \phi_1^-) - \omega^2 k^2 D_2 (|B|^2 \phi_1^+ + |A|^2 \phi_1^-)$$

$$+ \text{terms proportional to } E^3. \tag{2.24}$$

In the following, a Fourier decomposition will eliminate terms proportional to E^3, which would have been taken care of by inclusion of $\tilde{\phi}_3$. The coefficients D_1 and D_2 are given by

$$D_1 = \frac{\cosh 4kh + 8 - 2 \tanh^2 kh}{8 \sinh^4 kh}, \tag{2.25}$$

$$D_2 = \frac{-(16 \sinh^4 kh + 4 \tanh^2 kh)}{8 \sinh^4 kh}, \tag{2.26}$$

and have the deep-water asymptotes ($kh \to \infty$) of 1 and -2, respectively, in agreement with the results of Benney (1962) and Roskes (1976). Noting that the

left-hand side of (2.15) is a linear operator on ϕ_1, we then arrive at decoupled equations for ϕ_1^+ and ϕ_1^- given by

$$\phi_{1tt}^+ - \nabla_h \cdot (CC_g \nabla_h \phi_1^+) + (\omega^2 - k^2 CC_g)\phi_1^+ + 2\omega\left\{k\phi_{2x}' - \frac{k^2}{2\omega \cosh^2 kh}\phi_{2t}'\right\}\phi_1^+ + \omega^2 k^2 (D_1 |A|^2 + D_2 |B|^2)\phi_1^+ = 0, \quad (2.27a)$$

$$\phi_{1tt}^- - \nabla_h \cdot (CC_g \nabla_h \phi_1^-) + (\omega^2 - k^2 CC_g)\phi_1^- - 2\omega\left\{k\phi_{2x}' + \frac{k^2}{2\omega \cosh^2 kh}\phi_{2t}'\right\}\phi_1^- + \omega^2 k^2 (D_1 |B|^2 + D_2 |A|^2)\phi_1^- = 0. \quad (2.27b)$$

The change in sign of the terms $k\phi_{2x}'$ is related to the different directions of propagation of ϕ_1^+ and ϕ_1^-. Since D_2 is always < 0, while D_1 is > 0, it is apparent that the presence of a reflected-wave component ϕ_1^- weakens the effect of nonlinear self-interaction in the incident-wave component. Parabolic approximations governing A and B follow by neglecting time dependence for purely harmonic motion, and further by assuming that $O(|A_{xx}|) \ll O(k|A_x|)$ as in Kirby & Dalrymple (1983). The decoupled parabolic equations are then given by (following the method of Kirby & Dalrymple 1983)

$$2ikCC_g A_x + 2k(k-k_0)CC_g A + i(kCC_g)_x A + (CC_g A_y)_y - \omega^2 k^2 \left(D_1 |A|^2 + D_2 |B|^2 + \frac{2}{\omega k}(\phi_2')_x\right) A = 0, \quad (2.28)$$

and

$$2ikKCC_g B_x - 2k(k-k_0)CC_g B + i(kCC_g)_x B - (CC_g B_y)_y + \omega^2 k^2 \left(D_1 |B|^2 + D_2 |A|^2 - \frac{2}{\omega k}(\phi_2')_x\right) B = 0, \quad (2.29)$$

where k_0 is a constant wavenumber based on a reference depth h_0 and defining the reference phase function $k_0 x - \omega t$, and with A and B now defined according to

$$\phi_1^+ = -\frac{ig}{2\omega} A\, e^{i(k_0 x - \omega t)} + *; \quad \phi_1^- = -\frac{ig}{2\omega} B\, e^{i(-k_0 x - \omega t)} + *.$$

These equations are sufficient for modelling the propagation of the individual components ϕ_1^+ and ϕ_1^-, including their nonlinear interaction; however, we have not yet achieved a coupling capable of predicting the appearance of a gradually reflected component ϕ_1^-. This coupling is achieved in the following section.

2.3. *Effect of reflected wave and mass transport on the nonlinear dispersion of the incident wave*

The effect of reflected-wave components and induced flow on the third-order dispersion of the incident wave may be examined explicitly in the case of one-directional propagation over topography varying only in the direction of propagation. In this case, we may integrate (2.23) after neglecting time dependence to obtain

$$\phi_{2x}' = -\frac{gk}{2\omega h}(|A|^2 - |B|^2) + \text{constant}, \quad (2.30)$$

where the integration constant represents an externally imposed flow which is set to zero. Assuming that $|B| < |A|$; i.e. that ϕ_1^- represents a small wave arising owing

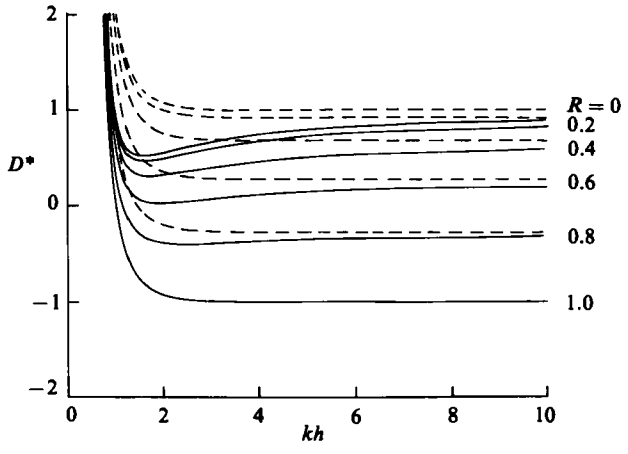

FIGURE 1. Variation of D^* with kh and reflection coefficient R: ——, including wave-induced return flow; – – –, neglecting wave-induced return flow.

to reflection, and taking $R = |B|/|A|$ to represent a reflection coefficient, the governing equation for the incident wave may be written as

$$2\mathrm{i}kCC_{\mathrm{g}}A_x + \mathrm{i}(kCC_{\mathrm{g}})_x A - \omega^2 k^2 D^* |A|^2 A = 0, \tag{2.31}$$

where

$$D^* = D_1 + D_2 R^2 - \frac{g}{\omega^2 h}(1 - R^2). \tag{2.32}$$

The last term in D^* represents the effect of wave-induced return flow balancing the shoreward mass flux of the waves. Since $D_2 < 0$ for all kh, the generation of a reflected component reduces the dispersive effect of nonlinearity. Conversely, increasing reflection tends to reduce the effect of the wave-induced return current, as the mass flux of the reflected wave tends to balance the flux of the incident wave.

Figure 1 gives plots of $D^*(kh, R)$ for a range $0 \leqslant R \leqslant 1$, with and without current effects included. It is noted that, for all reasonably small values of kh, the mean current has a noticeable effect on D^*, with the effect becoming pronounced for $kh \lesssim 4$. It is also apparent that the reflected wave can act to cancel entirely the amplitude dispersion of the incident wave, with the critical value given by

$$R_{\mathrm{c}} = \left\{\frac{g/\omega^2 h - D_1}{g/\omega^2 h + D_2}\right\}^{\frac{1}{2}}. \tag{2.33}$$

Neglecting current effects, this becomes

$$R_{\mathrm{c}} = \left\{-\frac{D_1}{D_2}\right\}^{\frac{1}{2}}, \tag{2.34}$$

which is defined for all kh and approaches $2^{-\frac{1}{2}}$ as $kh \to \infty$. When current is included, R_{c} is undefined for $kh \leqslant 0.649$; the deep-water asymptotic value is unaffected. A plot of R_{c} with and without currents is given in figure 2. Since it is apparent that the effect of the wave-induced flow can significantly alter the coefficient of the nonlinear term for values of kh small enough to give significant depth-change effects over a short spatial scale, in §4 we investigate the effect of retaining or dropping the current in a one-dimensional example, eliminating ϕ'_{2x} as was done here. The general problem of coupling between A, B and ϕ'_{2x} in two dimensions is left to a subsequent study.

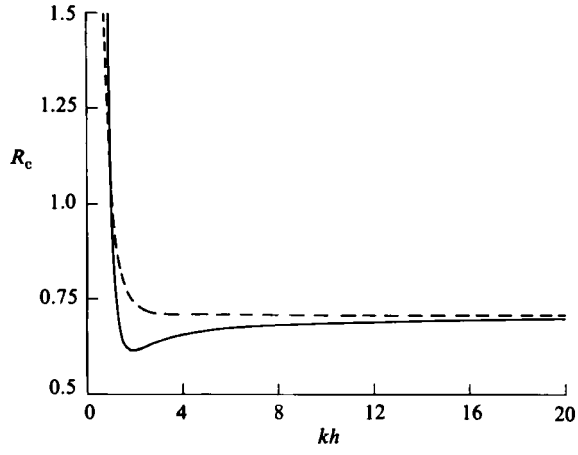

FIGURE 2. Critical reflection coefficient R_c for $D^* = 0$: ——, – – –, as in figure 1.

The results of the present study may be further checked by comparison with previous work on standing waves. It is well known that nonlinear standing waves of a given frequency may be longer or shorter than their linear counterparts, depending on the relative water depth. Tadjbakhsh & Keller (1960) have provided theoretical results which indicate that the point of transition, where the nonlinear and linear waves have equivalent lengths, occurs at a relative depth $h/L \approx 0.17$, where L is the wavelength. In the present context, this transition occurs when $D^* = 0$ for $R = 1$; the solution of (2.32) for this case gives $kh = 1.022$ or $h/L = 0.163$, which is lower than the value predicted by Tadjbakhsh & Keller. This discrepancy is due to the presence of the uniform set-down component of b_2 in (2.21). This uniform surface shift would not be allowed for a wave in a closed container (the case studied previously) due to mass-conservation requirements. Altering the theory to account for this restriction changes the expressions for b_2 and γ_2 to

$$b_2 = -\frac{1}{g}\phi'_{2t} + \frac{k\cosh 2kh}{2\sinh 2kh}\{AB^*E_+E_-^* + *\}, \tag{2.35}$$

and

$$\gamma_2 = -gk\frac{2\cosh 2kh - 1}{2\sinh 2kh}\{ABE_+E_- + *\} + gk\frac{|A|^2 + |B|^2}{2\sinh 2kh}. \tag{2.36}$$

This shift in reference level has a minor effect on the interaction coefficients D_1 and D_2, which are now given by

$$D_1 = \frac{\cosh 4kh + 8}{8\sinh^4 kh}, \tag{2.37}$$

$$D_2 = \frac{-(16\sinh^4 kh + 2\tanh^2 kh)}{8\sinh^4 kh}. \tag{2.38}$$

The revised solution to (2.32) is given by $kh = 1.058$ or $h/L = 0.168$, in agreement with the previous results. The factor ω_2, which represents the distortion to the wave frequency for a fixed wavelength in Tadjbakhsh & Keller, may be written in the present notation as

$$\omega_2 = \tfrac{1}{4}\omega D^*,$$

and the agreement between the two theories is seen to be complete.

2.4. *Extension to the case of rapid bed undulations*

The theory derived to this point is limited in application to waves propagating over mild bed slopes, with slope parameter μ presumed to be of $O(\epsilon^2)$ in order to separate nonlinear and bottom-slope effects. Reflections from such mild slopes are likely to be extremely weak in intermediate water depth. Therefore, it is desirable to incorporate the ability to model the effect of rapidly undulating, small-amplitude bed features following Kirby (1985). We thus add a bed amplitude parameter $k\delta$ to the list of $O(\mu)$ parameters, where δ represents the local deviation of the bed from a corresponding mild-slope bottom. If we retain the scaling assumptions used to this point, terms like δA, $\delta_x A$, etc. will still be of $O(\epsilon^3)$; the addition of this feature will not affect the amplitude dispersion and interaction with the wave-induced mean flow at the highest order of magnitude (ϵ^3) retained here. We therefore consider the extension of the linear-wave Lagrangian formulation to incorporate the features of Kirby (1985). The nonlinear terms are unaffected and may be retained intact from §2.2.

Defining the total water depth as in Kirby (1985), we have

$$h' = h - \delta, \tag{2.39}$$

where h varies slowly with lengthscale μ, and where δ may vary rapidly but has amplitude scale μ. Following (2.1), the Lagrangian for the inviscid motion may be written as

$$L = \int_{-h'}^{\eta} \rho\{\phi_t + \tfrac{1}{2}(\nabla_h \phi)^2 + \tfrac{1}{2}(\phi_z)^2 + gz\}\,\mathrm{d}z \tag{2.40}$$

We now expand the Lagrangian about $z = -h$ and retain the $O(\epsilon^2)$ contributions to the linear motion:

$$L = \frac{g\eta^2}{2} + \eta\phi_t|_{z=0} + \int_{-h}^{0} \tfrac{1}{2}(\nabla_h \phi)^2\,\mathrm{d}z - \tfrac{1}{2}(\nabla_h \phi)^2\,\delta|_{z=-h} + \int_{-h}^{0} \tfrac{1}{2}(\phi_z)^2\,\mathrm{d}z - \tfrac{1}{2}(\phi_z)^2\,\delta|_{-h}. \tag{2.41}$$

We now introduce

$$\phi = f_1(\mu x, z)\,\tilde{\phi}_1(x, t), \tag{2.42}$$

where f_1 is given in (2.5). Making the substitutions and integrating gives

$$L = \tfrac{1}{2}g\eta^2 + \eta\tilde{\phi}_t + \left(\frac{CC_g}{g}\right)\tfrac{1}{2}(\nabla_h \tilde{\phi})^2 + \left(\frac{\omega^2 - k^2CC_g}{g}\right)\tfrac{1}{2}\tilde{\phi}^2 - \frac{\delta}{\cosh^2 kh}\,\tfrac{1}{2}(\nabla_h \tilde{\phi})^2. \tag{2.43}$$

Taking variations of L with respect to $\tilde{\phi}$ and η and eliminating η leads to the modified wave equation given by Kirby (1985):

$$\tilde{\phi}_{tt} - \nabla_h \cdot (CC_g \nabla_h \tilde{\phi}) + (\omega^2 - k^2CC_g)\,\tilde{\phi} + \frac{g}{\cosh^2 kh}\,\nabla_h \cdot (\delta \nabla_h \tilde{\phi}) = O(\epsilon, \mu^2). \tag{2.44}$$

The nonlinear model follows, to $O(\epsilon^3)$, by adding the {N.L.T.} (2.24) to the modified equation (2.44).

3. The coupled parabolic equations

The desired set of coupled equations is derivable in a a large number of ways (see McDaniel 1975; Corones 1975; Radder 1979 and Liu & Tsay 1983 for examples) involving the application of a splitting matrix to the second-order wave equation. In order to extend the results of Kirby (1985) to nonlinear waves, we retain the added

term for bed undulations derived above. Restricting attention to harmonic waves and substituting

$$\phi_1 = \hat{\phi}\,\mathrm{e}^{-\mathrm{i}\omega t}; \quad \phi^+ = \hat{\phi}^+\,\mathrm{e}^{-\mathrm{i}\omega t}; \quad \phi^- = \hat{\phi}^-\,\mathrm{e}^{-\mathrm{i}\omega t} \tag{3.1}$$

into (2.15), we write

$$(\hat{\phi})_{xx} + p^{-1}p_x(\hat{\phi})_x + \gamma^2\hat{\phi} = N_1\hat{\phi}^+ + N_2\hat{\phi}^-, \tag{3.2}$$

where, to leading order,

$$p = CC_g - \frac{4\omega\Omega'\delta}{k}, \quad p^{-1} = (CC_g)^{-1}\left[1 + 4\left(\frac{\Omega'}{C_g}\right)\delta\right] + O(\mu^2), \tag{3.3a,b}$$

$$\Omega' = \frac{gk}{4\omega\cosh^2 kh}, \tag{3.3c}$$

$$\gamma^2\hat{\phi} = k^2\left\{\left(1 + 4\left(\frac{\Omega'}{C_g}\right)\delta\right)\hat{\phi} + \frac{1}{k^2CC_g}(CC_g\hat{\phi}_y)_y - \frac{4}{k^2}\left(\frac{\Omega'}{C_g}\right)(\delta\hat{\phi}_y)_y\right\}, \tag{3.3d}$$

$$N_1 = \frac{\omega^2k^2}{CC_g}\left(D_1|A|^2 + D_2|B|^2 + \frac{2}{\omega k}\phi'_{2x}\right), \tag{3.4a}$$

and

$$N_2 = \frac{\omega^2k^2}{CC_g}\left(D_1|B|^2 + D_2|A|^2 - \frac{2}{\omega k}\phi'_{2x}\right). \tag{3.4b}$$

We remark that the pseudo-operator γ is constructed without isolating a refraction factor k/k_0, alleviating the need for making the assumption that

$$1 - \left(\frac{k}{k_0}\right)^2 \ll 1 \tag{3.5}$$

when performing the binomial expansion of the pseudo-operator (Liu & Tsay 1983). This assumption may be violated drastically for waves propagating through regions with large depth variations.

We follow the heuristic scheme of Kirby (1985) for obtaining the parabolic equations. Let

$$\hat{\phi}^+_x = \mathrm{i}\gamma\hat{\phi}^+ + F(\hat{\phi}^+, \hat{\phi}^-) + \alpha N_1\hat{\phi}^+, \tag{3.6a}$$

$$\hat{\phi}^-_x = -\mathrm{i}\gamma\hat{\phi}^- - F(\hat{\phi}^+, \hat{\phi}^-) + \beta N_2\hat{\phi}^-, \tag{3.6b}$$

where F, α, and β are undetermined. α and β are chosen so as to eliminate nonlinear terms from the coupling term F, leading to equations of the form of (2.28)–(2.29). Repeated substitution of (3.6) in (3.2) then leads to

$$\alpha = -\beta = -\frac{\mathrm{i}}{2k} \tag{3.7a}$$

and

$$F = -\left\{\frac{(kCC_g)_x}{2kCC_g} - \left(\frac{\Omega'}{C_g}\right)\delta_x\right\}(\hat{\phi}^+ - \hat{\phi}^-), \tag{3.7b}$$

where we have retained terms only to $O(\mu, \epsilon)$ and have used the fact that

$$CC_g\{N_1\hat{\phi}^+, -N_2\hat{\phi}^-\}_x \approx \mathrm{i}kCC_g\{N_1\hat{\phi}^+, N_2\hat{\phi}^-\} + O(\epsilon^3, \mu) \tag{3.8a}$$

and

$$(CC_g)_x\{N_1\hat{\phi}^+, N_2\hat{\phi}^-\} \cong O(\epsilon^3, \mu). \tag{3.8b}$$

The resulting coupled parabolic equations are then given by

$$\hat{\phi}^+_x - \mathrm{i}k\hat{\phi}^+ - \frac{\mathrm{i}}{2kCC_\mathrm{g}}(CC_\mathrm{g}\hat{\phi}^+_y)_y + \frac{(kCC_\mathrm{g})_x}{2kCC_\mathrm{g}}(\hat{\phi}^+ - \hat{\phi}^-) - 2\mathrm{i}k\left(\frac{\Omega'}{C_\mathrm{g}}\right)\delta\hat{\phi}^+ + \frac{2\mathrm{i}}{k}\left(\frac{\Omega'}{C_\mathrm{g}}\right)(\delta\hat{\phi}^+_y)_y - \left(\frac{\Omega'}{C_\mathrm{g}}\right)\delta_x(\hat{\phi}^+ - \hat{\phi}^-) + \frac{\mathrm{i}}{2k}N_1\hat{\phi}^+ = 0 \quad (3.9)$$

and

$$\hat{\phi}^-_x + \mathrm{i}k\hat{\phi}^- + \frac{\mathrm{i}}{2kCC_\mathrm{g}}(CC_\mathrm{g}\hat{\phi}^-_y)_y - \frac{(kCC_\mathrm{g})_x}{2kCC_\mathrm{g}}(\hat{\phi}^+ - \hat{\phi}^-) + 2\mathrm{i}k\left(\frac{\Omega'}{C_\mathrm{g}}\right)\delta\hat{\phi}^- - \frac{2\mathrm{i}}{k}\left(\frac{\Omega'}{C_\mathrm{g}}\right)(\delta\hat{\phi}^-_y)_y + \left(\frac{\Omega'}{C_\mathrm{g}}\right)\delta_x(\hat{\phi}^+ - \hat{\phi}^-) - \frac{\mathrm{i}}{2k}N_2\hat{\phi}^- = 0. \quad (3.10)$$

Equations of the form (2.28)–(2.29) are recovered by making the substitutions

$$\hat{\phi}^+ = \frac{-\mathrm{i}g}{\omega}A\,\mathrm{e}^{\mathrm{i}k_0x}; \quad \hat{\phi}^- = \frac{-\mathrm{i}g}{\omega}B\,\mathrm{e}^{-\mathrm{i}k_0x}, \quad (3.11)$$

yielding

$$2\mathrm{i}kCC_\mathrm{g}A_x + 2k(k-k_0)CC_\mathrm{g}A + (CC_\mathrm{g}A_y)_y + 2\omega\Omega'[2k\delta - \mathrm{i}\delta_x]A - \frac{4\omega\Omega'}{k}(\delta A_y)_y + \mathrm{i}(kCC_\mathrm{g})_xA - CC_\mathrm{g}N_1A = \{\mathrm{i}(kCC_\mathrm{g})_x - 2\mathrm{i}\omega\Omega'\delta_x\}B\,\mathrm{e}^{-2\mathrm{i}k_0x} \quad (3.12)$$

and

$$2\mathrm{i}kCC_\mathrm{g}B_x - 2k(k-k_0)CC_\mathrm{g}B - (CC_\mathrm{g}B_y)_y - 2\omega\Omega'[2k\delta + \mathrm{i}\delta_x]B + \frac{4\omega\Omega'}{k}(\delta B_y)_y + \mathrm{i}(kCC_\mathrm{g})_xB + CC_\mathrm{g}N_2B = \{\mathrm{i}(kCC_\mathrm{g})_x - 2\mathrm{i}\omega\Omega'\delta_x\}A\,\mathrm{e}^{2\mathrm{i}k_0x}. \quad (3.13)$$

Equations (3.12)–(3.13) may be used in an iterative fashion to calculate the evolution of the amplitude envelopes A and B. The numerical scheme used in subsequent sections is based on the Crank–Nicolson method, with each equation solved for the entire domain using the scheme of Yue & Mei (1980), after which iteration between the equations is performed according to the method provided by Liu & Tsay (1983). Details are thus omitted.

Three forms of coupling between (3.12) and (3.13) are apparent. The waves interact nonlinearly through the coefficients N_1 and N_2. Secondly, there is a mild-slope coupling through the $(kCC_\mathrm{g})_x$ terms on the right-hand sides. Since kCC_g is presumed to be slowly varying, $(kCC_\mathrm{g})_x$ will usually be a smooth, $O(\mu)$ quantity and the factors $\mathrm{e}^{\pm 2\mathrm{i}k_0x}$ will provide a near-cancellation due to the rapid oscillation. The third form of interaction is through the factor δ_x on the right-hand side. This quantity is again of $O(\mu)$; however, the rapid undulation of δ will, in resonant cases, provide a cancellation of the $\mathrm{e}^{\pm 2\mathrm{i}k_0x}$ factors, leading to strong coupling between incident and reflected waves.

The present method of derivation does not lead to coupling due to transverse diffusion terms because of the approximation used to obtain the factor $(\gamma p)_x$ used in F (3.7*b*). This coupling appears in the models of Radder (1979) and Liu & Tsay (1983) in the form of third-derivative terms and is sensibly neglected by Liu & Tsay in their applications of the model.

4. Effect of mass transport terms on nonlinear reflection: normal incidence on one-dimensional topography

As a test of the effect of nonlinearity on the partial reflection process, we first study the reflection of normally incident waves propagating over a continuous, one-dimensional region of varying depth. This reduction of the problem allows for the direct integration of the forced-wave equation (2.23) as given by (2.30). Neglect of the integration constant forces the wave-induced return flow to balance the net mass transport, and is thus consistent with the situation of wave-tank experiments. Further, we note that the generation of free long waves should be absent from the problem owing to the lack of wavelike modulations in the amplitude envelopes.

The choice of computational examples which exhibit significant reflection over a short spatial scale is difficult in this problem, since water depth would have to be relatively shallow in order for an isolated topographic variation with an extent of one to two wavelengths to have a significant effect on the incident wave. For example, the numerical example chosen by Liu & Tsay (1983) was run for a water depth at infinity corresponding to $kh = 0.42$. The range of admissible waveheights yielding an Ursell parameter of a permissible size for the Stokes theory to be valid is thus severely constrained. Likewise, the linear transition studied by Booij (1983) covered a range of depths corresponding to $0.2 \leqslant kh \leqslant 0.6$, again too small to be of particular use.

For the purposes of this study we have chosen to consider the case of reflection from an isolated patch of sinusoidally undulating topography as studied recently by Davies & Heathershaw (1983).

The topography is given by $h(x) = h_1$ and

$$\delta(x) = \begin{cases} 0 & (x < 0), \\ D \sin(2\pi x/l) & (0 \leqslant x \leqslant nl), \\ 0 & (x > nl), \end{cases} \tag{4.1}$$

where l is the ripple length and n is the number of ripples. The topography is illustrated in figure 3. For a fixed geometry given by $D = 5$ cm and $l = 100$ cm, Davies & Heathershaw conducted a large number of experiments for the ranges $0.08 \leqslant D/h_1 \leqslant 0.4$ (obtained by varying h_1) and $1 \leqslant n \leqslant 10$. The lower range of D/h_1 corresponds to $kh = O(1)$ at the peak reflection; these experiments are thus useful in the present context. The full linear wave theory presented by Davies & Heathershaw predicts a strong reflection for the value

$$\frac{2k}{\lambda} = 1, \tag{4.2}$$

where $\lambda = 2\pi/l$ or $L_{\text{wave}}(= 2\pi/k) = 2l$, due to Bragg scattering of the incident wave by the ripple patch. This reflection peak is amplified owing to a resonant interaction between the incident- and reflected-wave components and the undular bottom. Kirby (1985) has presented a numerical solution of the linearized elliptic problem with rapid bed undulations in order to compare with the linear perturbation solution of Davies & Heathershaw. The numerical solution was seen to give a good reproduction of the analytic results. Comparisons have been made using the 'corrected theory' of Davies & Heathershaw, which is obtained by imposing an energy balance on their solution in cases where reflection is large.

The theoretical results of Davies & Heathershaw were used as a check of the iterative scheme (3.12)–(3.13) in its linearized form. Results for the case illustrated

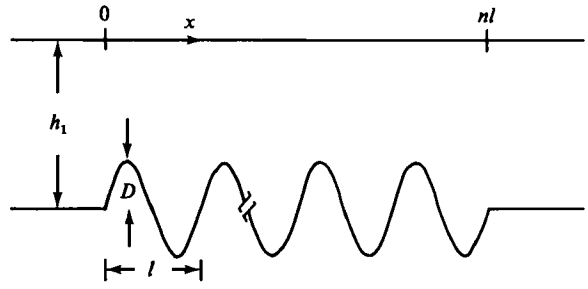

FIGURE 3. Topography for one-dimensional-model tests.

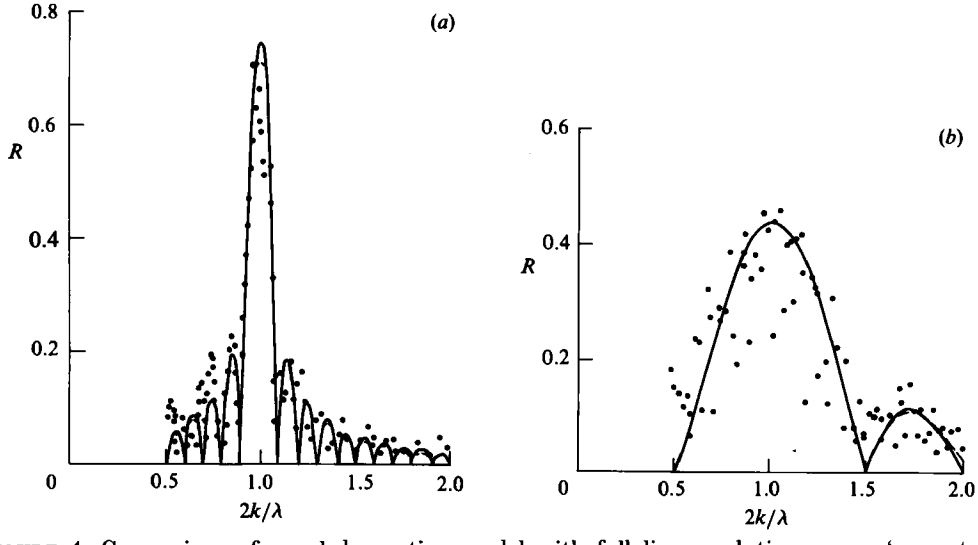

FIGURE 4. Comparison of coupled-equation model with full linear solution: ——, 'corrected' solution, Davies & Heathershaw; – – –, present undular-bed solution; data, Davies & Heathershaw. (*a*) $D/h_1 = 0.16$, $n = 10$. (*b*) $D/h_1 = 0.32$, $n = 2$.

in figure 3 of Kirby (1985) ($D/h_1 = 0.16$, $n = 10$) and for a new case $D/h_1 = 0.32$, $n = 2$ respectively were computed using the coupled parabolic equations and a grid spacing $\Delta x = l/20$. The reflection coefficients for both cases are shown in figure 4. The peak reflection coefficient R obtained using the parabolic model (including rapid depth variation) is slightly less than the values predicted by the 'corrected' theory of Davies & Heathershaw for the $D/h_1 = 0.16$ case and within plotting accuracy for the $D/h_1 = 0.32$ case. For $2k/\lambda > 2.0$ the number of points per incident wavelength drops below 20, and some reduction in the reflection coefficient was noted. A further reduction in grid spacing to $\Delta x = l/10$ caused a reduction of the reflected-wave amplitude at $2k/\lambda = 1$ of 6.6% for the case with $n = 10$. Therefore the value of $\Delta x = l/20$ was used for all subsequent runs.

We now use the nonlinear form of the parabolic equation to study the reflection process. Tests were performed using the geometry of figure 4 (*a*) ($D/h_1 = 0.16$); results are presented in figure 5 for incident-wave steepness $\epsilon = 0.2$. A plot of Ursell number $U_r = (A_0/h)/(kh)^2$ for this case is given in figure 6. The plot indicates that, for the chosen value of ϵ, results of the Stokes-wave model are only roughly valid for the region $2k/\lambda < 1$. For small values of $2k/\lambda$ (large wavelength) it is anticipated that the incident-wave phase speed is overestimated. This would have the effect of over-

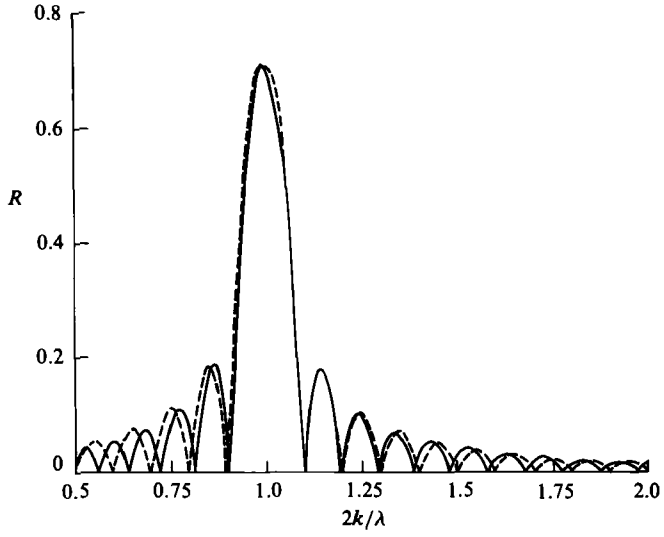

FIGURE 5. Variation of R for $\epsilon = 0.2$; $n = 10$, $D/h_1 = 0.16$: ——, nonlinear; – – –, linear.

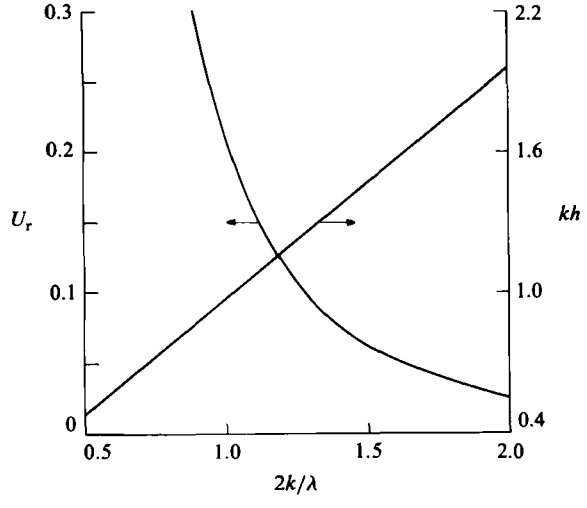

FIGURE 6. Variation of Ursell Number U_r and relative depth kh for example of figure 5.

emphasizing the differences between the linear and nonlinear reflection curves in this range.

The curve for nonlinear reflection shown in figure 5 is for the case of no wave-induced current. It was found that the presence or absence of the wave-induced flow had no significant effect on the reflection process; the corresponding curve for reflection including mean flows is thus not included. This result may be partially explained by considering a simplified set of equations taken from (2.28)–(2.29):

$$\mathrm{i}A_x - \frac{\omega U}{CC_g} A = 0, \tag{4.3}$$

$$\mathrm{i}B_x - \frac{\omega U}{CC_g} B = 0, \tag{4.4}$$

where depth is constant and amplitude dispersion is neglected. The quantity U may represent the wave-induced return flow or a small flow imposed by boundary conditions. Oscillatory solutions of constant amplitude are given by

$$\{A(x), B(x)\} = \{a, b\}\, \mathrm{e}^{\mathrm{i}k'x}, \tag{4.5}$$

where

$$k' = -kU/C_{\mathrm{g}}, \tag{4.6}$$

so that

$$\phi_1^+ = \frac{-\mathrm{i}g}{2\omega}\, a\, \mathrm{e}^{\mathrm{i}[k(1-U/C_{\mathrm{g}})x-\omega t]} + \text{c.c.}, \tag{4.7a}$$

$$\phi_1^- = \frac{-\mathrm{i}g}{2\omega}\, b\, \mathrm{e}^{\mathrm{i}[-k(1+U/C_{\mathrm{g}})x-\omega t]} + \text{c.c.} \tag{4.7b}$$

For simplicity, b may be set equal to a; the resulting standing wave may be written as

$$\phi_1 = \frac{2ga}{\omega} \cos kx \cos\left\{\frac{kU}{C_{\mathrm{g}}}x + \omega t\right\}, \tag{4.8}$$

which reduces to the usual stationary form at $U \to 0$. It is clear that the stationary component $\cos(kx)$ is unaffected by the presence of U; the relation between the wave envelope and topography is thus unaltered.

The effect of nonlinearity is thus limited to the lengthening of the incident wave (for small R) with respect to the topography at fixed ω (or k). For large $2k/\lambda$, the effect is a downshift of the maxima and minima of R which increases with increasing ϵ. It is remarked that, for large R, the incident waves may be shortened by nonlinearity; the shift in the pattern of R would then be expected to be towards higher values of $2k/\lambda$.

In the present example, the large reflection coefficient at the peak $2k/\lambda$ causes a significant weakening of the nonlinear dispersion in the incident wave on the upwave side of the ripple patch. Referring to figure 1, we see that a reflection coefficient of 0.6–0.7 would lead to an effective nonlinear parameter D^* with values in the neighbourhood of 0. Nonlinearity thus has little effect on the reflection process when reflection is strong; this is born out by the result of little or no shift in peak value or location of R for this example. This conclusion is partially supported by the experimental results of Davies & Heathershaw, who saw little or no effect of varying wave steepness on peak reflection, up to the point of breaking in the incident wave.

5. Two-dimensional topography

As mentioned in the previous section, the availability of examples which satisfy the mild-slope assumption and still provide significant reflection over several wavelengths is limited to shallow water, for which the present Stokes-wave model is not applicable. Cases where the requirement of intermediate water depth (or Ursell number $U_{\mathrm{r}} \ll 1$) is satisfied tend to exhibit too small a reflection to be of interest here. For example, the present model indicates that the reflection upwave of the isolated shoal in the data of Berkhoff, Booij & Radder (1982) is limited to approximately 1–2 % of the incident wave height.

In order to take advantage of the relatively strong reflections caused by the undulating topography studied in the previous section, we construct a two-dimensional patch of ripples of finite extent in the x- and y-directions. Ripples with length l are aligned with crests parallel to the y-axis. The patch is symmetric about the x-axis

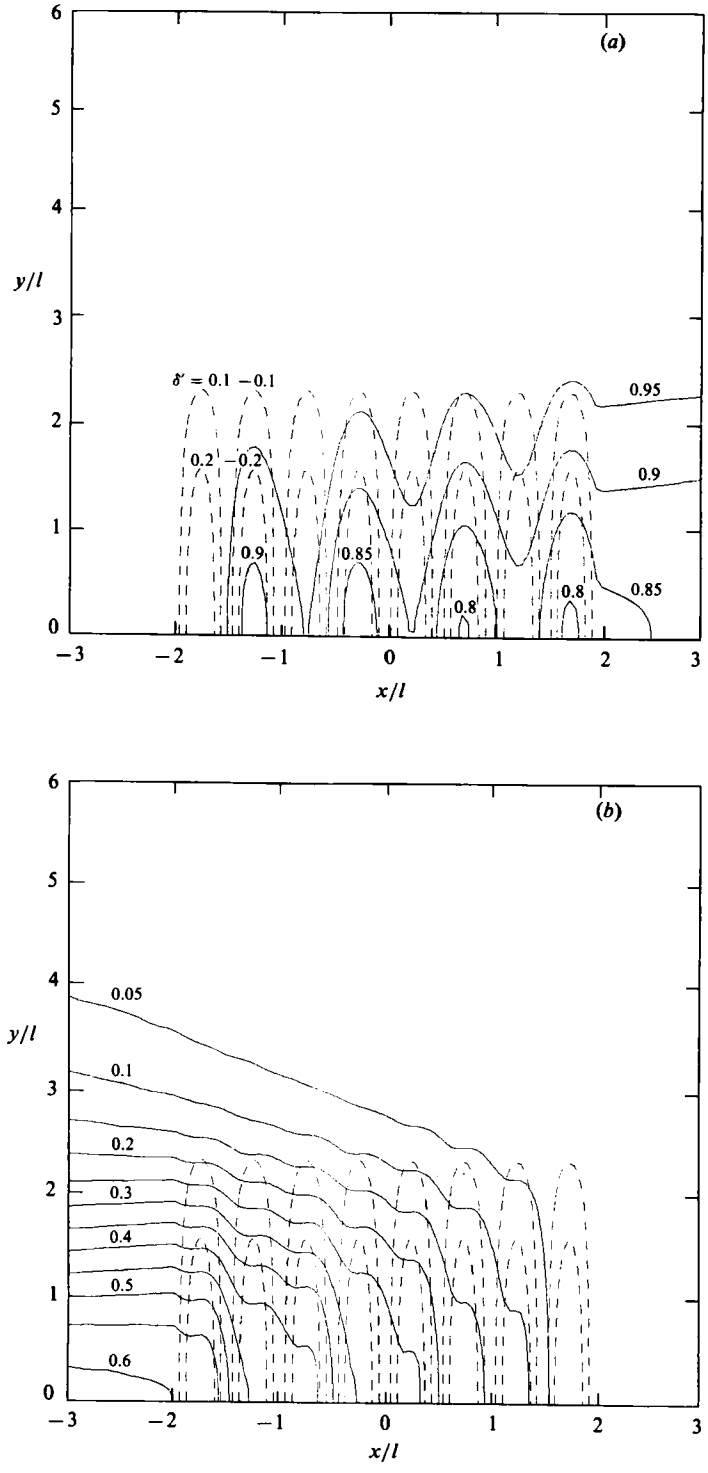

FIGURE 7 (*a*, *b*). For caption see facing page.

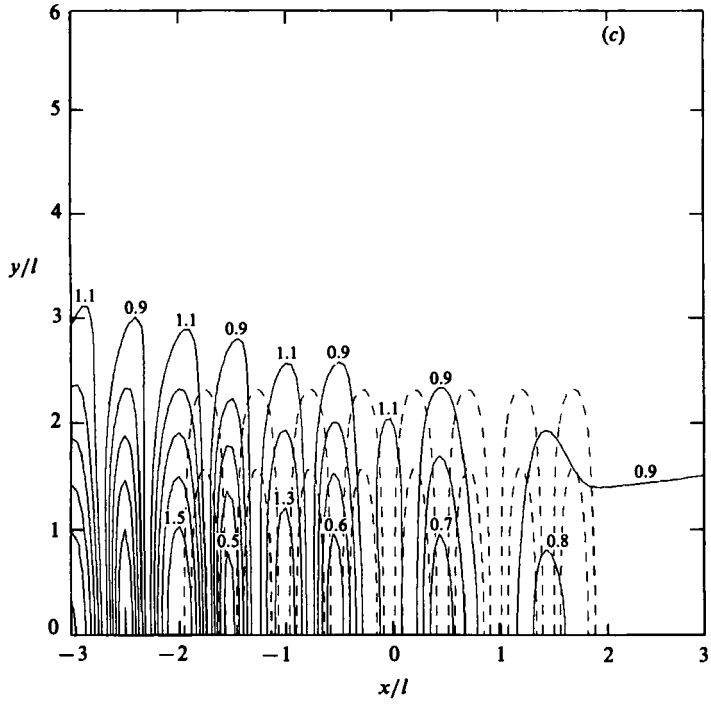

FIGURE 7. Normalized amplitude contours: linear wave. $n = 4$, $l = 1$, $D/h_1 = 0.3$, $h_1 = \pi^{-1}$, $2k/\lambda = 1$: ——, amplitude contours; – – –, depth contours $\delta' = \delta/h_1$. (*a*) Incident wave $|A/A_0|$, (*b*) reflected wave $|B/A_0|$, (*c*) total wavefield $|\eta/A_0|$.

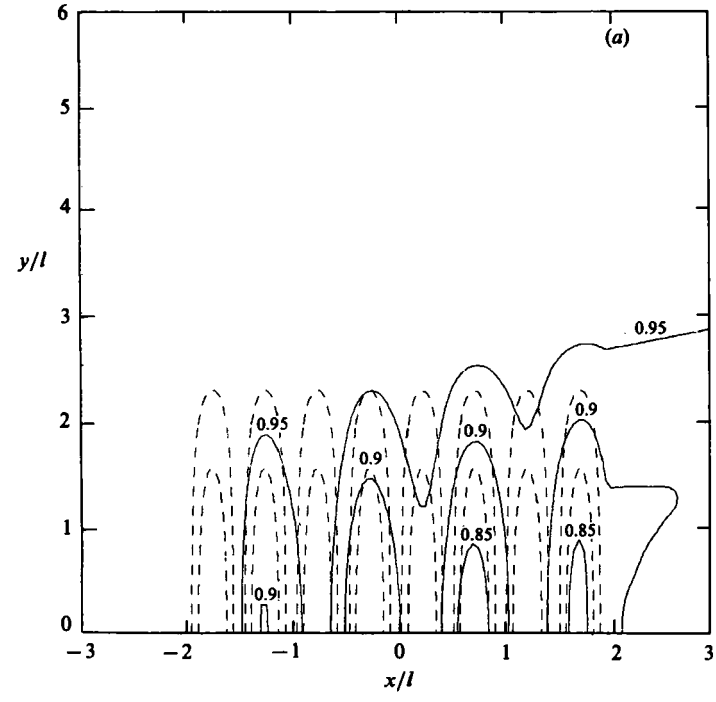

FIGURE 8(*a*). For caption see next page.

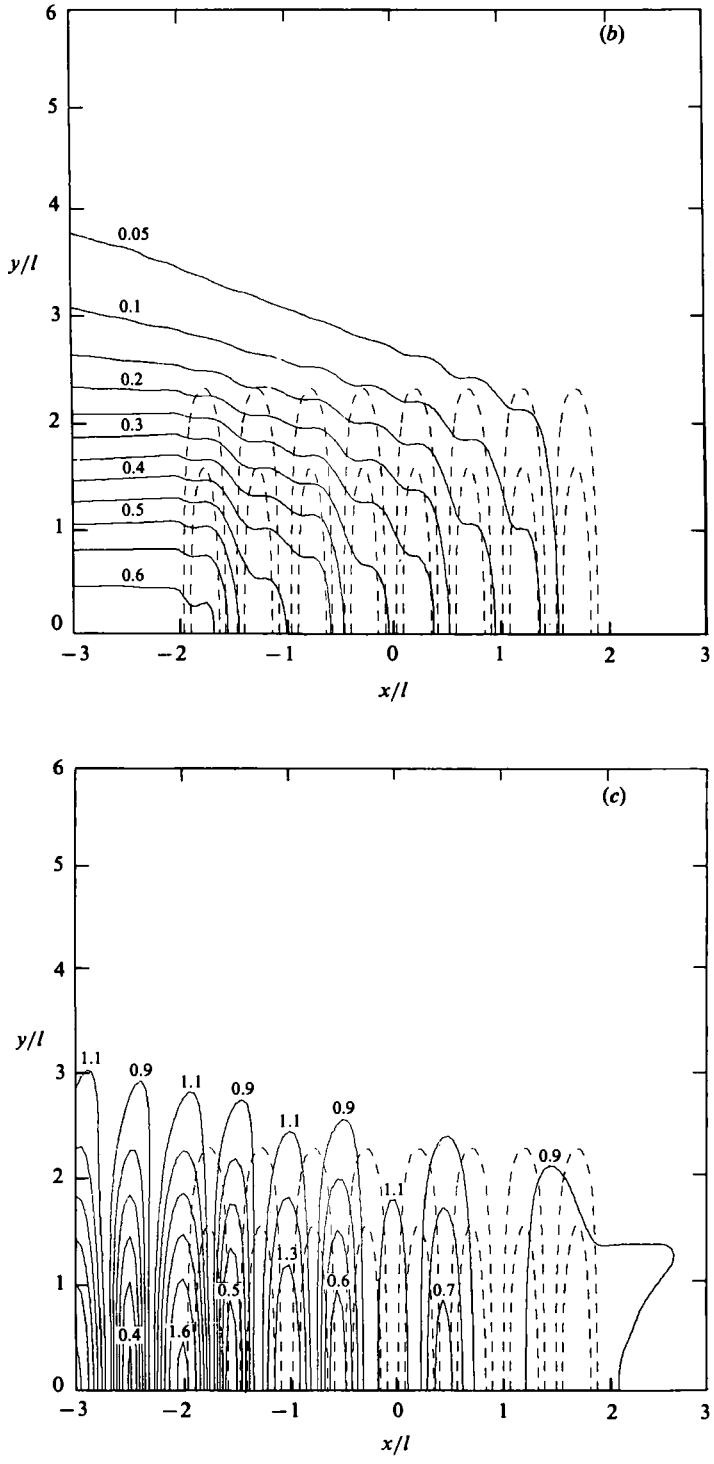

FIGURE 8. Normalized amplitude contours: nonlinear wave $\epsilon = 0.2$. $n = 4$, $l = 1$, $D/h_1 = 0.3$, $h_1 = \pi^{-1}$, $2k/\lambda = 1$: ——, amplitude contours; – – –, depth contours $\delta' = \delta/h_1$. (*a*) Incident wave $|A/A_0|$, (*b*) reflected wave $|B/A_0|$, (*c*) total wavefield $|\eta/A_0|$.

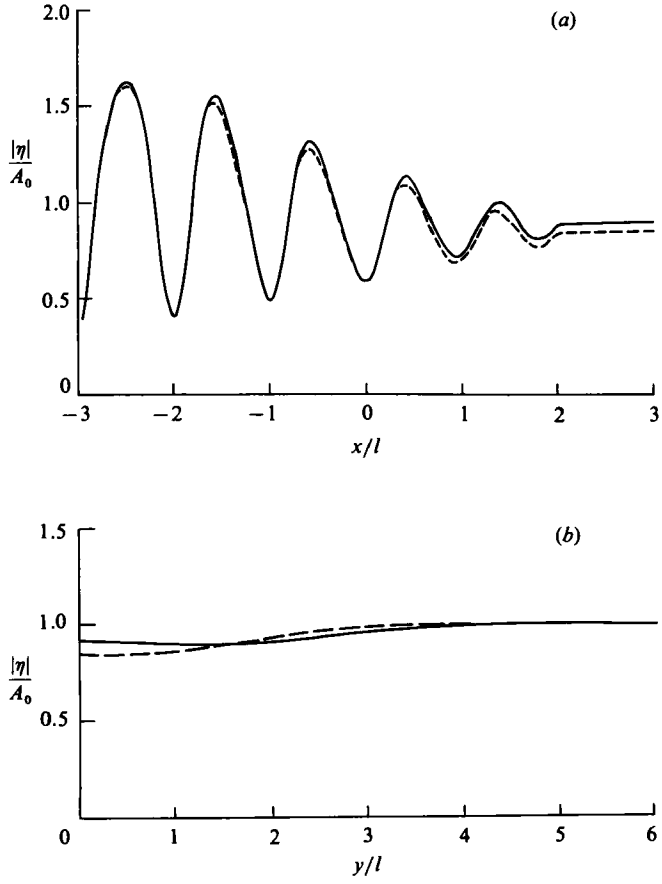

FIGURE 9. Amplitude $|\eta|/A_0$. $n = 4$, $D/h_1 = 0.3$, $h_1 = \pi^{-1}$: – – –, linear waves; ——, nonlinear waves, $\epsilon = 0.2$. (*a*) Amplitude along centreline $y = 0$, (*b*) amplitude along downwave transect $x = 3l$.

with dimensions $nl \times 2nl$ in x and y, where n is the number of ripples as before. The topography is specified according to $h(x,y) = h_1$ and

$$\delta(x, y) = \begin{cases} D \sin(\lambda x) \cos(\lambda y/4n), & |x| \leqslant \frac{1}{2}nl, \quad |y| \leqslant nl; \\ 0, & |x| > \frac{1}{2}nl, \quad |y| > nl, \end{cases} \tag{5.1}$$

where h_1 is the depth away from the ripple patch. The computational domain is taken to be $\{x, y \,|\, |x| \leqslant (n+2)\frac{1}{2}l,\ 0 \leqslant y \leqslant 2nl\}$, with $A(-(n+2)\frac{1}{2}l, y) = A_0$ specified as the incident-wave amplitude. Computations were run with $2k/\lambda = 1$, $D/h_1 = 0.3$ and a far-field relative depth $kh_1 = 1$, giving $h_1 = \pi^{-1}$ with $l = 1$. The Ursell number $U_r = (a/h_1)/(kh_1)^2$ and wave steepness $\epsilon = ka$ are thus both given by πA_0 for the incident wave.

Results are shown for the case of $n = 4$ in figures 7 and 8. Figure 7 gives results for the linear case, with normalized amplitude $|A/A_0|$ given in 7(*a*), $|B/A_0|$ in 7(*b*) and the total-wave-amplitude envelope $|\eta/A_0|$ in 7(*c*). In figure 8, results are for the case of $\epsilon = u_r = 0.2$. A comparison of the figures indicates some differences in the transmitted wavefield over and downwave of the ripple patch, with the amplitude downwave of the last ripple being increased in the nonlinear case, indicating the greater tendency towards diffraction effects due to nonlinearity. This result is

consistent with the phenomenon of self-defocusing as demonstrated by Kirby & Dalrymple (1983) and, further, is in agreement with Yue's (1980) results showing that diffraction of waves into a shadowed region proceeds more quickly in the nonlinear case. The reflected-wave amplitudes are quite similar for both cases, with a minor increase in peak amplitude at the upwave end of the ripple patch being noted in the nonlinear case.

Comparisons of normalized amplitude for the total wavefield along $y = 0$ and along $x = 3l$ are given in figures 9(*a*) and (*b*) respectively, for the linear and nonlinear cases. Differences are largely confined to an increase in transmitted wave height downwave of the ripple patch in the nonlinear case, as discussed above.

The effect of diffraction in the present example may be estimated simply. If we take the peak reflection along the centreline to be approximately $R = 0.6$ from figures 7 or 8(*b*), we conclude that the transmitted amplitude downwave of the patch should be

$$T = (1 - R^2)^{\frac{1}{2}} = 0.8.$$

This value is in rough agreement with the linear result but underestimates the nonlinear value of $T \approx 0.9$, again indicating the more rapid effects of diffraction in the nonlinear case.

6. Discussion

In this study we have utilized a variational principle to develop a wave equation governing the propagation of Stokes waves in a varying domain, after which use is made of a splitting method to provide coupled equations for forward- and back-scattered components of an initially plane incident wave propagating over uneven topography.

The restriction to Stokes waves and the resulting constraints on water depth relative to the incident wavelength makes it difficult to develop computational examples which describe a significant reflection process arising over a short spatial scale. Under the mild-slope conditions and the restriction to intermediate water depths, it is likely that the gradual reflection process would be apparent only over fairly long spatial scales. The inclusion of the undular bed formulation of Kirby (1985) has allowed for the study of reflection by relatively rapid, small-amplitude bed features.

For the case of shallower water, the Stokes-wave formulation is no longer valid, and recourse must be made to appropriate equations such as the Boussinesq equations. The parabolic approximation for a spectrum of steady (in time) forward-scattered waves in the shallow-water regime has been provided by Liu, Yoon & Kirby (1985); the development of a model for partial reflection in this case is straightforward, owing to the lack of nonlinear coupling between incident and reflected waves at second order, and will be the subject of a further investigation. Also of special interest is the case where the incident-wave amplitude is modulated in space and time. The treatment of 'groupy' waves is not approachable using the reduced wave equation of §3; however, the general time-dependent model (2.15) may form the basis of such an approach, after further accounting for terms arising owing to possible fast spatial modulations of $O(\epsilon)$ in the amplitude functions. In this case, the 'mild-slope' nature of the model may be retained by continuing the restriction that depth variations be restricted to $O(\mu = \epsilon^2)$; the terms in the equation which depend on gradients of the physical domain would be unaltered.

This work was supported in part by the Office of Naval Research, Coastal Sciences Program. This is contribution no. 461 of the Marine Sciences Research Center, State University of New York at Stony Brook, where this work was commenced.

Appendix A. Integrals of f functions

The integrals I are defined as the integral over total depth of an integrand f, and may be expanded according to

$$I = \int_{-h}^{\eta} f\,\mathrm{d}z = \int_{-h}^{0} f\,\mathrm{d}z + \eta f|_0 + \eta^2 \frac{f_z|_0}{2} + \frac{\eta^3 f_{zz}|_0}{6} + \ldots$$
$$= I' + \eta I'' + \eta^2 I''' + \eta^3 I^{\mathrm{iv}} + \ldots. \tag{A 1}$$

Substitution of the expansion (2.4*b*) for η yields (2.7). The individual integrals and required components are given by

$$I_1 = \int_{-h}^{\eta} f_1\,\mathrm{d}z; \quad I_1'' = 1, \quad I_1''' = \frac{\omega^2}{2g}, \quad I_1^{\mathrm{iv}} = \tfrac{1}{6}k^2, \tag{A 2}$$

$$I_{1,1} = \int_{-h}^{\eta} f_1^2\,\mathrm{d}z; \quad I_{1,1}' = \frac{CC_{\mathrm{g}}}{g}, \quad I_{1,1}'' = 1, \quad I_{1,1}''' = \frac{\omega^2}{g}, \tag{A 3}$$

$$I_{1,1}^z = \int_{-h}^{\eta} f_{1z}^2\,\mathrm{d}z; \quad I_{1,1}^{z'} = \frac{\omega^2 - k^2 CC_{\mathrm{g}}}{g}, \quad I_{1,1}^{z''} = \frac{\omega^4}{g^2}, \quad I_{1,1}^{z'''} = \frac{k^2\omega^2}{g}, \tag{A 4}$$

$$I_2 = \int_{-h}^{\eta} f_2\,\mathrm{d}z; \quad I_2' = \frac{\cosh kh}{k\sinh^3 kh}, \quad I_2'' = \frac{\cosh 2kh}{\sinh^4 kh}, \quad I_2''' = \frac{2k\cosh kh}{\sinh^3 kh}, \tag{A 5}$$

$$I_{1,2} = \int_{-h}^{\eta} f_1 f_2\,\mathrm{d}z; \quad I_{1,2}'' = \frac{\cosh 2kh}{\sinh^4 kh}, \tag{A 6}$$

$$I_{1,2}^z = \int_{-h}^{\eta} f_{1z} f_{2z}\,\mathrm{d}z; \quad I_{1,2}^{z''} = \frac{4k^2}{\sinh^2 kh}, \tag{A 7}$$

$$I_{2,2} = \int_{-h}^{\eta} f_2^2\,\mathrm{d}z; \quad I_{2,2}' = \frac{\sinh 2kh}{2k\sinh^8 kh}\left\{\sinh^2 kh + \frac{C_{\mathrm{g}}}{C}\right\}, \tag{A 8}$$

$$I_{2,2}^z = \int_{-h}^{\eta} f_{2z}^2\,\mathrm{d}z; \quad I_{2,2}^{z'} = \frac{2k\sinh 2kh}{\sinh^8 kh}\left\{\cosh^2 kh - \frac{C_{\mathrm{g}}}{C}\right\}. \tag{A 9}$$

Appendix B. Components of the primitive Lagrangian L

The Lagrangian L is expanded as a series in powers of the wave-steepness parameter ϵ without regard to the relative size of the modulation parameter μ. After expanding η and the integrals I in (2.6), the individual components of L in (2.8) are given by (after dividing out the constant density ρ)

$$L_0 = -\tfrac{1}{2}gh^2, \tag{B 1}$$

$$L_1 = I_1'\tilde{\phi}_{1t}, \tag{B 2}$$

$$L_2 = \tfrac{1}{2}g\eta_1^2 + I_1''\eta_1\tilde{\phi}_{1t} + I_{1,1}'\tfrac{1}{2}(\nabla_{\mathrm{h}}\tilde{\phi}_1)^2 + I_{1,1}^{z'}\tfrac{1}{2}(\tilde{\phi}_1)^2 + h(\phi_{2t}' - \gamma_2) + I_2'\tilde{\phi}_{2t}, \tag{B 3}$$

$$L_3 = g\eta_1(\eta_2 + b_2) + I_1''(\eta_2 + b_2)\tilde{\phi}_{1t} + I_1'''\eta_1^2\tilde{\phi}_{1t} + \eta_1(\phi_{2t}' - \gamma_2)$$
$$+ I_2''\eta_1\tilde{\phi}_{2t} + I_{1,1}''\eta_1\tfrac{1}{2}(\nabla_{\mathrm{h}}\tilde{\phi}_1)^2 + I_{1,2}'\nabla_{\mathrm{h}}\tilde{\phi}_1\cdot\nabla_{\mathrm{h}}\tilde{\phi}_2 + I_1'\nabla_{\mathrm{h}}\tilde{\phi}_1\cdot\nabla_{\mathrm{h}}\phi_2'$$
$$+ I_{1,1}^{z''}\tfrac{1}{2}\eta_1\tilde{\phi}_1^2 + I_{1,2}^{z'}\tilde{\phi}_1\tilde{\phi}_2, \tag{B 4}$$

$$L_4 = \tfrac{1}{2}g(\eta_2+b_2)^2+(\eta_2+b_2)\,\phi'_{2_t}+2I'''_1\,\eta_1(\eta_2+b_2)\,\tilde{\phi}_{1_t}+I^{\mathrm{iv}}_1\eta_1^3\tilde{\phi}_{1_t}$$
$$+I''_2(\eta_2+b_2)\tilde{\phi}_{2_t}+I'''_2\,\eta_1^2\tilde{\phi}_{2_t}+I''_{1,1}(\eta_2+b_2)\tfrac{1}{2}(\nabla_{\mathrm{h}}\tilde{\phi}_1)^2$$
$$+I'''_{1,1}\,\eta_1^2\tfrac{1}{2}(\nabla_{\mathrm{h}}\tilde{\phi}_1)^2+I'_{2,2}\tfrac{1}{2}(\nabla_{\mathrm{h}}\tilde{\phi}_2)^2+h\tfrac{1}{2}(\nabla_{\mathrm{h}}\phi'_2)^2+I''_{1,2}\eta_1\nabla_{\mathrm{h}}\tilde{\phi}_1\cdot\nabla_{\mathrm{h}}\tilde{\phi}_2$$
$$+\eta_1\nabla_{\mathrm{h}}\tilde{\phi}_1\cdot\nabla_{\mathrm{h}}\phi'_2+I'_2\nabla_{\mathrm{h}}\tilde{\phi}_2\cdot\nabla_{\mathrm{h}}\phi'_2+I^{z''}_{1,1}(\eta_2+b_2)\tfrac{1}{2}(\tilde{\phi}_1)^2+I^{z'''}_{1,1}\eta_1^2\tfrac{1}{2}\tilde{\phi}_1^2$$
$$+I^{z'}_{2,2}\tfrac{1}{2}(\tilde{\phi}_2)^2+I^{z''}_{1,2}\eta_1\tilde{\phi}_1\tilde{\phi}_2-\gamma_2(\eta_2+b_2). \tag{B 5}$$

Appendix C. General form for $O(\epsilon^3)$ term in wave equation

The term {N.L.T.} in (2.15) is given here in terms of $\tilde{\phi}_1$, $\tilde{\phi}_2$, (η_2+b_2) and ϕ'_2. The first-order surface η_1 has been eliminated through use of (2.9). Further, we have made use of the fact that

$$(\tilde{\phi}_1,\tilde{\phi}_2)_{tt}=(-\omega^2\tilde{\phi}_1,-4\omega^2\tilde{\phi}_2)+O(\mu), \tag{C 1}$$

$$\nabla_{\mathrm{h}}^2(\tilde{\phi}_1,\tilde{\phi}_2)=(-k^2\tilde{\phi}_1,-4k^2\tilde{\phi}_2)+O(\mu), \tag{C 2}$$

for both progressive and standing waves. {N.L.T.} is then given by

$$\{\text{N.L.T.}\}=\left\{\frac{-gk^2}{\cosh^2 kh}(\eta_2+b_2)+\frac{2\omega^2k^2}{g^2}(\tilde{\phi}_{1_t})^2-k^4\tanh^2 kh(\tilde{\phi}_1)^2\right.$$
$$\left.-k^2\tanh^2 kh(\nabla_{\mathrm{h}}\tilde{\phi}_1)^2-\frac{8k^2}{\sinh^2 kh}\tilde{\phi}_{2_t}\right\}\tilde{\phi}_1$$
$$+\left\{-2k\tanh kh\,\eta_{2_t}+\frac{4k^2(1-2\sinh^2 kh)}{\sinh^4 kh}\tilde{\phi}_2+\frac{k\tanh kh}{g}(\nabla_{\mathrm{h}}\tilde{\phi}_1)^2_t\right\}\tilde{\phi}_{1_t}$$
$$+\left\{g\nabla_{\mathrm{h}}(\eta_2+b_2)+\frac{k\tanh kh}{g}\nabla_{\mathrm{h}}(\tilde{\phi}^2_{1_t})-\frac{\cosh 2kh}{\sinh^4 kh}\nabla_{\mathrm{h}}\tilde{\phi}_{2_t}\right\}\cdot\nabla_{\mathrm{h}}\tilde{\phi}_1$$
$$+\left\{-2\nabla_{\mathrm{h}}\phi'_2-\frac{2\cosh 2kh}{\sinh^4 kh}\nabla_{\mathrm{h}}\tilde{\phi}_2\right\}\cdot\nabla_{\mathrm{h}}\tilde{\phi}_{1_t}, \tag{C 3}$$

where we have substituted for all I-values from Appendix A.

REFERENCES

Benney, D. J. 1962 Nonlinear gravity wave interactions. *J. Fluid Mech.* **14**, 577–584.

Berkhoff, J. C. W. 1972 Computation of combined refraction–diffraction. In *Proc. 13th Intl Conf. Coastal Engng, Vancouver*, vol. 2, pp. 471–490. ASCE.

Berkhoff, J. C. W., Booij, N. & Radder, A. C. 1982 Verification of numerical wave propagation models for simple harmonic linear waves. *Coastal Engng* **6**, 255–279.

Corones, J. 1975 Bremmer series that correct parabolic approximations. *J. Math. Anal. Appl.* **50**, 361–372.

Davies, A. G. & Heathershaw, A. D. 1983 Surface wave propagation over sinusoidally varying topography: theory and observation. *Rep.* 159, Institute of Oceanographic Sciences.

Dysthe, K. B. 1974 A note on the application of Whitham's method to nonlinear waves in dispersive media. *J. Plasma Phys.* **11**, 63–76.

Kirby, J. T. 1983 Propagation of weakly-nonlinear surface water waves in regions with varying depth and current. Ph.D. dissertation, University of Delaware, Newark.

Kirby, J. T. 1986 A general wave equation for waves over rippled beds. *J. Fluid Mech.* **162**, 171–186.

Kirby, J. T. & Dalrymple, R. A. 1983 A parabolic equation for the combined refraction–diffraction of Stokes waves by mildly varying topography. *J. Fluid Mech.* **136**, 453–466.

KIRBY, J. T. & DALRYMPLE, R. A. 1984 Verification of a parabolic equation for propagation of weakly-nonlinear waves. *Coastal Engng* **8**, 219–232.

LIU, P. L.-F. & MEI, C. C. 1976 Water motion on a beach in the presence of a breakwater. 1. Waves. *J. Geophys. Res.* **81**, 3079–3094.

LIU, P. L.-F. & TSAY, T.-K. 1983 On weak reflection of water waves. *J. Fluid Mech.* **131**, 59–71.

LIU, P. L.-F. & TSAY, T.-K. 1984 Refraction–diffraction model for weakly nonlinear water-waves. *J. Fluid Mech.* **141**, 265–274.

LIU, P. L.-F., YOON, S. B. & KIRBY, J. T. 1985 Nonlinear refraction–diffraction of waves in shallow water. *J. Fluid Mech.* **153**, 184–201.

LUKE, J. C. 1967 A variational principle for a fluid with a free surface. *J. Fluid Mech.* **27**, 395–397.

MCDANIEL, S. T. 1975 Parabolic approximations for underwater sound propagation. *J. Acoust. Soc. Am.* **58**, 1178–1185.

RADDER, A. C. 1979 On the parabolic equation method for water-wave propagation. *J. Fluid Mech.* **95**, 159–176.

ROSKES, G. J. 1976 Nonlinear multiphase deep-water wavetrains. *Phys. Fluids* **19**, 1253–1254.

TADJBAKHSH, I. & KELLER, J. B. 1960 Standing surface waves of finite amplitude. *J. Fluid Mech.* **8**, 442–451.

TSAY, T.-K. & LIU, P. L.-F. 1982 Numerical solution of water-wave refraction and diffraction problems in the parabolic approximation. *J. Geophys. Res.* **87**, 7932–7940.

TSAY, T.-K. & LIU, P. L.-F. 1983 A finite element model for wave refraction and diffraction. *Appl. Ocean Res.* **5**, 30–37.

WHITHAM, G. B. 1967 Non-linear dispersion of water waves. *J. Fluid Mech.* **27**, 399–412.

YUE, D. K.-P. 1980 Numerical study of Stokes wave diffraction at grazing incidence. Sc.D. dissertation, Massachusetts Institute of Technology.

YUE, D. K.-P. & MEI, C. C. 1980 Forward diffraction of Stokes waves by a thin wedge. *J. Fluid Mech.* **99**, 33–52.